PRELIMINARY STUDY OF A HIGHER ENERGY PRE-INJECTOR FOR THE CERN PS

J. Huguenin, U. Tallgren, M. Weiss

European Organization for Nuclear Research
Geneva, Switzerland

INTRODUCTION

The improvement program of the CERN PS Linac foresees a possible reconstruction of the first tank. In connection with this we felt it interesting to study the influence of an increase in the pre-injector energy. The results from a first study presented here indicate interesting advantages to be gained, particularly if we could push up the pre-injector energy drastically, e.g. by a factor 4 - 5. Technological aspects will put a limit to such a change and a fresh look at the problem connected with the accelerating tube, H.T. supply and the ion source has been made. Lay-out, reliability and operational aspects have also been discussed. We conclude that it certainly seems worth while to carry out a more detailed study of the feasibility of a higher energy pre-injector in view of the potential advantages to be gained for the Linac beam.

The PS Linac Beam

The Linac beam characteristics are usually represented with a certain number of diagrams belonging to various phase planes (two transverse and one longitudinal). In the transverse phase planes (y,y') and (z,z') the accelerated current is related to the corresponding emittances E_y and E_z respectively. A typical set of curves $I = f(E)$ for the PS Linac and pre-injector is given in Fig. 1.

It is seen that a deterioration occurs when passing from 0,5 MeV to 50 MeV, its main part lying in the region 0,5 - 10 MeV, i.e. at the beginning of acceleration. We shall examine this region with respect to various pre-injector energies and focusing structures, keeping the RF properties as they are in the present linac.

For convenience in Fig. 2 the energy increase in tank I is given as function of cell number and β.

ANALYSIS OF LINAC PERFORMANCE WITH RESPECT TO DIFFERENT PRE-INJECTOR ENERGIES

The results of studies of the linac performance calculated for various pre-injector energies, are presented in the form of diagrams. For the sake of comparison, the same mean accelerating field E_0, stable phase angle φ_s and drift-tubes bore radii as with the actual Linac are kept throughout. The q value (ratio of the betatron to synchrotron frequency) is 0.75.

1st. Group of diagrams : wiggle factor analysis; Linac acceptance.

The betatron amplitude function is denoted with β in order to distinguish it from the relativistic factor β. The diagrams were calculated in the system (r,p), where r is the position coordinate and p the corresponding normalized momentum:

$$p = \frac{m \frac{dr}{dt}}{m_0 c} .$$

Fig. 3 shows the wiggle factor for the focusing structures + - and + + - - . Both, higher injection energy and + - structure, have clear advantages.

Fig. 4 gives the increase in drift-tube bore radius along the 1st Linac tank. Fig. 5 gives the variation in β_{max} up to 3 MeV. This curve gives information also about the changes in beam radius, which is $\propto \beta_{max}^{1/2}$.

Fig. 6 is drawn with the aid of Figs. 4 and 5 and shows the Linac acceptance increase when going to higher pre-injector energies and changing from + + - - to + - focusing structure. E.g., when passing from + + - - structure and 0,5 MeV to + - structure and 3 MeV, the Linac acceptance increases in each of the transverse phase planes ~ 4 times.

2nd. Group of diagrams : quadrupole lens strength; accelerating field defocusing.

Fig. 7 compares the quadrupole lens strength calculated for the two types of focusing structures and q value of 0,75. The calculations were carried out in the normalized (r,p) system, where δ (presented on the diagram) is in fact the thin lens strength multiplied by $\beta\gamma$.

Fig. 8 gives the variation of the magnetic gradient from 0.5 to 3 MeV. It is easy to show that this variation is $\propto (\beta\gamma)^{3/2}$ for q = const.

Fig. 9 gives the ratio of gap defocusing to the quadrupole strength, both in thin lens approximation. The averaged gap defocusing force is expressed with the modified Bessel function of the first order of which only the linear term (in r) is retained :

$$F_r = \frac{e\,E\,T\,\pi \sin\varphi_s}{\beta\,\gamma^2\lambda}\,r$$

E .... mean accelerating field
T .... transit time factor
φ_s .... stable phase angle
λ = c/f , f = RF frequency
r .... distance from axis.

To be consistent in the normalized (r,p) system, the "gap defocusing strength" to be compared with the quadrupole strength δ is :

$$\frac{F_r}{m_r} \cdot \frac{\gamma}{fc} = \chi^2 \frac{\gamma}{fc} .$$

It is possible to demonstrate that the curve of Fig. 9 falls approximately $\propto (\beta)^{-1/2}$. That is to say the gap defocusing becomes less important as the energy increases. Therefore, at higher energies, the Linac focusing structure is less time dependent.

The time dependence of the focusing structure makes the linac acceptance as well as the linac emittance vary with the phase angle. If this time dependence can be reduced, there are 2 consequences:

- the common area of the acceptances belonging to various phase angles is increased,
- the overall linac emittance (i.e. the sum of all instantaneous emittances) is decreased.

More detailed quantitative results of the above effects are not available for the moment.

Another way of making the Linac focusing structure less time dependent is to increase the q value. A higher q value calls for stronger magnetic gradients in quadrupoles. However, at higher energies, this becomes easier to achieve because the gradients required for focusing diminish (compare Fig. 8).

The PS Linac works at its low energy end with a q of 0.75, safely chosen between half integer and integer resonant values. Other possible working values would be 1.25, 1.75, etc.

In Fig. 10 the quadrupole lens strengths are represented as function of q for an energy of 2.5MeV. Comparing this figure to Fig. 7, we see that the quadrupole strength for q = 1.25 and + - structure at 2.5 MeV is roughly 1.4 times bigger than that for q = 0.75, + + - - structure and 0.5 MeV. This does not present a difficulty as the drift-tubes at 2.5 MeV are longer, and the above requirement can be fulfilled with magnetic gradients even smaller than in the present first drift-tubes. As far as the maximum magnetic field is concerned, it is practically the same in both cases, due to the increased drift-tube bore radii at 2.5 MeV.

3rd. Group of diagrams : transit time factor; bunching efficiency.

The transit time factor varies when going from the beam center towards the beam boundary, making the acceleration non uniform across the beam. Fig. 11 gives an idea of this variation. For equal beam emittance, the curve belonging to the + - structure is more favourable due to smaller beam envelope wiggles.

The essential feature of Fig. 11 is that both curves tend to unity as the energy increases. Therefore progressively in the linac the acceleration becomes more uniform over the beam cross section.

Fig. 12 shows the beam bunching at 0.53 MeV (0.53 MeV is roughly the PS Linac pre-injector energy) for different currents. The buncher voltage is 17 KV, giving to the beam an energy spread of roughly one third of the available Linac bucket height. The effect of bunching is accompanied by an increase in beam radius, see Fig. 12a, coming from :

a) defocusing action of the buncher gap,
b) space charge action.

The above figures were obtained with the aid of a computer programme recently written by F. Vermeulen (Ref. 1). For the moment, the lenses existing between the buncher and Linac were not taken into account. The inclusion of focusing into the calculations (in preparation) will certainly alter the results, but the present picture could still be retained for a comparative study.

Figs. 13 and 13a show the same as Figs. 12 and 12a, only for 2.5 MeV pre-injector energy. The buncher voltage applied (56 KV) is such as to keep the beam energy spread in the same ratio to the respective bucket extension as at 0.5 MeV. The initial beam diameter at 2.5 MeV is taken 50% bigger than that at 0.5 MeV, according to the increased drift-tube bore radius. The beam was assumed to have a rotational symmetry.

The diagrams show clearly the general tendency: with higher beam intensities, the maximum longitudinal bunching decreases and occurs later, whilst the corresponding beam radius increases.

It seems to be convenient, especially for the sake of comparison, to formulate a unique expression for bunching efficiency. This expression has to contain the longitudinal grouping of particles as well as the transversal spreading. The transversal spreading due to space charge is especially interesting. We defined therefore a "bunching quality factor" as :

$$\eta = \frac{\left(\frac{I}{I_{tot}}\right)_{max} \pm \Delta\Phi}{\frac{r_{I_{max}} - r_{o_{max}}}{r_{o_{max}}}}$$

where $\left(\frac{I}{I_{tot}}\right)_{max \pm \Delta\Phi}$ represents the maximum relative amount of current within a certain longitudinal phase extension and

$\frac{r_{Imax} - r_{o_{max}}}{r_{o_{max}}}$ is the corresponding relative increase in beam radius with respect to the radius $r_{o_{max}}$, belonging to the no space charge case. This bunching quality factor is represented on Fig. 14 and can be considered as a provisional figure of merit of the bunching.

Conclusion

The present study is a first analysis of the advantages of a linac with a higher pre-injector energy.

Many of the numerical calculations were carried out by hand (mostly done by L. Nielsen, vacation student from the Technical University, Copenhagen). They will be followed by computer calculations, supplying us with more quantitative results.

Some advantages of a higher pre-injector energy are briefly summarized :

a) decrease of the ratio of overall linac emittance to the emittance for the phase stable particles,

b) better trapping efficiency,

c) increase in Linac acceptance (transverse),

d) more uniform acceleration across the beam,

e) smaller stray field aberrations in lenses,

f) easier Tank I design (the relativistic factor β increases in the actual Tank I 4.41 times, whilst in Tank II and III only 1.72 and 1.26 times respectively). Injecting at 2.5 MeV, β in Tank I would increase 1.98 times.

TECHNOLOGICAL ASPECTS

General

Technological problems will set a limit to the maximum obtainable energy. In particular, very high voltage holdoff will depend upon the insulation properties of the gaseous medium and on the voltage application time. This leads naturally to the introduction of two main solutions for each of the above criteria :

Criterium 1 a) Insulation at atmospheric pressure.
b) Insulation under compressed gas.

Criterium 2 a) DC high voltage.
b) Pulsed high voltage.

Criterium 1 can be applied either to the generator or to the tube independently, or to both at the same time. One can, for example, imagine a generator under compressed gas feeding an open air tube through a bushing and a cable.

Roughly speaking, the maximum practical limit of an open air structure can be set in our case at 1 MV in DC. Already at this voltage, which supposes interelectrode distances without potential division around 4 meters, the present Faraday cage would be too small. With a pulsed voltage this 1 MV limit could perhaps be extended towards higher voltage. For DC voltages above 1 MV, we must adopt a compressed gas solution, which requires probably that both tube and generator should be in the same tank : cables are available for voltages only up to 1,2 MV. In this case one can define two main solutions (Fig. 15). In the first, the tube is physically in parallel with the generator which supplies an identical voltage gradient for both. This is troublesome because the tube accelerating gradient has not much to do with the generator gradient : the accelerating gap itself should actually be shorter than the generator. We could then foresee a large diameter tube with re-entrant source and earth electrode. In addition,one cannot introduce a protective resistance, insulated for the total voltage between tube and generator. The advantage of the parallel solution is, on the other hand, that it can probably be made physically compact. In the second solution, tube and generator are in line, (Fig. 15) or at right angle (Fig. 19) and can be linked by a tubular element which can be either a protective resistance or a short-circuit, according to the needs. This solution allows a greater independence between the conception of tube and generator. This is also of importance for the interconnection between the firm in charge of the generator and the CERN people developing the tube.

The choice of gas and pressure could depend on the wishes of the HT supply manufacturer. The use of SF 6 will mean working at a pressure below 5 atm., the use of a mixture of, e.g. $CO_2 + N_2$, a pressure at least twice as high.

We have mentioned Criterium 2 because we think that for a pulse length of 100 to 200 μsec., sufficient for the future needs of the pre-injector, we are probably at the limit where a holdoff improvement, both in the vacuum and in the gas, could be found as compared with a DC solution. A careful study of this particular problem could be carried out at a given time.

Although it is difficult to split them up, we shall exmaine successively the problems connected with the tube, the generator, the source and other factors such as layout and operational aspects.

Accelerating Tube

Introduction. The following high voltage gradients represent the major problems :

a) Accelerating gradient.

b) Gradient on the insulating wall, on the vacuum side.

c) Gradient on the insulating wall, on the gas side.

If one could achieve three identical gradients, it means that the tube need have no re-entrant source or re-entrant ground-electrode, and the tube diameter could be small. On the contrary, if the gradient on the wall was inferior to the accelerating gradient, the source or/and the ground-electrode would need to be re-entrant. The advantages and disadvantages of these two geometries are shown in Table 1. Notice for example that the solution A of Table 1 was adopted for the new high gradient 550 KeV tube installed in the Linac. The research efforts had been concentrated on achieving the high acceleration gradient, leaving aside the problem of increasing the field along the insulating walls. This solution also allowed a great flexibility for future modifications of the accelerating gradient.

A few other problems to be solved are listed below :

d) Gradient inside the insulating material of the walls, in relation with a,b,c.

e) A leak-tight assembly process for the insulating rings (the pressure difference could reach a few atmospheres) and without organic vapours (for instance brazing techniques).

f) Proper potential distribution along the tube.

Accelerating Gradient. The mean accelerating gradiant of the present CPS pre-injector is about 5o kV/cm. Suppose for the moment that a gradient of this order of magnitude should be chosen for the proposed pre-injector, meaning for instance gaps of 40 cm for 2 MV and 60 cm for 3 MV. As far as we know, such gradients have never been obtained at those voltages but are aimed at (eg. HVEC, Ref. 21). The diagram Fig. 16 shows working voltage, maximum voltage, length and accelerating gradient of different accelerating tubes.

The vacuum hold-off of such tubes is limited by two phenomena, which can either be independent or related to each other : the breakdown and the electron loading. In this last case a back streaming electron current produces bremstrahlung X rays at the source end. This radiation ionizes the vessel compressed gas, producing a current which can reach prohibitive values. The loading starts at a well defined threshold voltage and rises with the 6th power of the voltage increase (Ref. 2). It varies also with the 6th power of the tube diameter (Ref. 3), the tube vacuum pressure (Ref. 4) and the contamination of the tube (Ref. 5). In order to eliminate this effect efforts have been under way for about fifteen years for preventing secondary electron production, electron acceleration over the whole tube length, X ray production. These techniques, using field reversal, inclined, tilted or scalloped electrodes, tapered diagrams, magnetic fields (Ref. 6 to 13) have allowed the building of tubes with a maximum voltage proportional to the length. Notice that in addition to the better HT hold-off and to the smaller generator loading, the elimination of the energetic γ rays represent a substantial advantage from the health physics point-of-view, and brings therefore considerable operational simplifications.

In spite of these different techniques, the achieved gradients are still well below 5o kV/cm. Nevertheless, it should be noted that the tubes built up to now have never been equipped with the electrode materials recently used at CERN for very high gradients and voltages between 500 and 800 kV :

- Titanium alloys for the Linac pre-injector (> 100 kV/cm at 600 kV at 10^{-6} ÷ 10^{-4} mm Hg)
- Anodised aluminium for electrostatic separators (100 kV/cm at 600 kV at 10^{-6} mm Hg).

As one knows, both materials have the property of having a negligible electron loading compared with conventional materials (Ref. 14, 15, 22).

Gradient on the insulating wall in vacuum. The hold-off on one tube insulator section can be studied rather independently of the total number of sections, with an appropriate screening of one section against external ions, electrons and γ rays. This protection is clearly easier to make than the screening of an assembly of accelerating gaps, which are inevitably linked together by the beam passage hole. The study of the behaviour of one insulator section individually should then lead to a maximum voltage proportional to the number of sections. The maximum gradient on the surface of insulators in vacuum depends mainly on following factors: insulator length, insulator material, insulator surface state, insulator shape, electrode material, electrode shape, especially at the negative junction, quality of insulator-electrode joint, especially at the negative junction. For example, the junction edge should be free of organic cement, which is most frequently present. Most conventional tubes assembled with such cement, after a certain working period, show organic deposits, having their origin at the junction. In the case of the new Linac pre-injector, where the araldite was completely masked, the porcelain shows no traces after two years of functioning, whereas the previous pre-injector porcelains, with a conventional cementing technique, had to be cleaned twice a year.

Equally the material of the electrodes around each insulating section should not vaporize too easily. Titanium, for example, which presents an excellent hold-off across a gap must be avoided near insulators if the local potential differences or energies are great because it sputters very easily. With a voltage per section of 40 kV, as in the new pre-injector, titanium was not producing troublesome vaporization. On the other hand, vaporization coming from the tube wall shielding has been noticed on insulators of the ion source, with a voltage difference of ~200 kV. This is an additional reason

for a complete optical screening of each section, protecting it not only against ions, electrons and γ rays as mentioned at the beginning of this paragraph, but also against metallic or other vaporization (source cathode oxides, etc.) coming from the tube centre. (Ref. 22).

Finally, we should consider that this protection, as well as the screening of insulators mentioned above, leads inevitably to local reinforcements of the mean electrical field. This means that a tube with non re-entrant electrodes will have local gradients greater than the acceleration gradient (see Table 1). This speaks in favour of a tube with re-entrant electrodes.

Gradient on the insulating wall in the gas. The maximum permissible local gradient on any negative electrode in the gas seems to be around 100 kV/cm. Above this value, cold emission occurs and can lead to breakdowns. A mean tube gradient of 50 kV/cm means that precautions must be taken so as not to go beyond the above cathode field. Nevertheless, certain makers of HT generators use an insulating distance between the HT electrode and the pressure tank of 40 cm for 2 MV and of 60 cm for 3 MV under 4 atm. of SF 6, i.e. a mean gradient of 50 kV/cm. Since this is for a gap without potential division, it seems that the realisation of 50 kV/cm along a tube with potential division is possible, even in the presence of insulators. A re-entrant tube will be, of course, easier to make.

HT Generators

DC generators. There does not seem to exist a major difficulty to get on the market supplies from 1 to 3 MV with reasonable characteristics i.e. required DC current, short and long term stability and suitable size. For instance longitudinal gradients of 1 MV/m are conventionaly used for Greinacher cascade type supplies.

Source and HT Terminal Equipment

General

The source should be able to produce more than 500 mA of beam current with high brilliance in pulses of up to 100 μs (multiturn injection) at a repetition rate of maximum one pulse per second. It is also evident that in order to get a reasonable pressurized system, we must suppress the present electronic platform and mount all the source electronics and its power generator in the high voltage terminal. This puts stringent requirements on size, power consumption and weight. The maximum permissible weight will depend on the lay-out of the pre-injector. The weight has to be taken either by the column or the HT generator, probably both, depending on whether a protective resistor is required between the HT generator and the column.

Duoplasmatron Ion Source

The PS Duoplasmatron (Ref. 16) has proved its value and can easily produce a high brilliance beam in the 0.5 - 1 A range. The present source and its electronics have an estimated weight of several hundred kg and a power consumption of > 3 kW. Further studies are required before one can assess to which limits power consumption and weight can be reduced.

RF Ion Source

A new RF ion source has been shortly described in a previous report (Ref. 17) (Fig. 17). This source has given beam currents of more than 500 mA. It is characterized by a two-step acceleration before the limiting outlet channel. Breakdown problems are therefore greatly diminished, which is an important factor for the lifetime of the source. At Nimrod an RF ion source has after removal of breakdown causes now been in operation without trouble for 10 000 hours (Ref. 18). It was shown (Ref. 17) that the emittance of an RF ion source is very small and should therefore be able to produce a high brilliance beam, provided that the initial emittance does not deteriorate later.

An example of what present day technology can do for us in order to reduce power consumption size and weight of the electronics, is given in Fig. 18 (Dimensions in mm).

It seems feasible to build a pulsed RF ion source producing a high brilliance beam of more than 500 mA which with its associated electronics would consume less than 500 W and weigh less than 50 kg.

Further experiments on determination of optimum electrode material and shape for the extraction system, life time studies and emittance measurements are evidently necessary before one can conclude that this source fulfills all of our requirements.

Power, Controls and Monitoring

Our present power generator on the electronic platform supplies slightly more than 3 kW. Evidently one would not be happy to include a generator of this size and weight in a pressurized system. However, if we can get away with a total power requirement around 500 W in the high voltage terminal, the size and weight get substantially reduced. For instance, present day AC car generators are compact, of low weight and are well suited to feed transistorized equipment.

For controls and monitoring we have a well established technique, making use of light emitting GaAs-diodes as transmitters and Foto-fet transistors as receivers (Ref. 19).

Reliability and Operational Aspects

The reliability aspect is a very important one, and will be further enhanced in future when the PS booster and the ISR rings are in operation. The inherent disadvantage of a pressurized system lies in its inaccessibility. On the other hand, the overall dimensions of the pre-injector will be greatly reduced which, apart from economical considerations, permit us to think in terms of two complete pre-injectors ready for operation.

At some existing pressurized pre-injectors (Ref. 20) one has achieved a minimum opening and closing time at a repair inside the system of the order of one hour. The maximum time at certain industrial installations, where gas drying is employed, can, however, be as high as 24 hours. The gas treatment plant must be well studied in order to minimize this time as much as possible.

The time required for an ion source change would mainly be determined by the gas handling time plus the time required for re-pumping and forming the column. A valve between the source and column would practically shorten this time to what is required for handling the pressurized gas. In case of hold-off difficulties in the accelerating tube and also for the first conditioning after a shut-down period, this valve would also be useful for testing the column separately without breaking the pre-injector vacuum to replace the source by a dummy plate.

Lay-out

It is too early to commit courselves to any particular lay-out. However, as an example we give on Fig. 19 one possible solution. The generator is vertical, which is of advantage from mechanical point-of-view for supporting its own weight as well as the source and HT terminal equipment. The column is shown horizontal, coming out level with the input end of the Linac. Since that solution actually belongs to the same family as solution b of Fig. 15, the gradient of the accelerating tube and the HT generator can be very different, e.g. 10 kV/cm for the generator and 50 kV/cm for the tube. As mentioned earlier, if we want to attain 50 kV/cm inside the accelerating tube, but not on the outside, we can do this by re-entrant electrodes, making the overall length of the tube longer. The top part of the pressurized vessel can be mounted with hydraulic lifting pistons, in order to reduce the access time for the HT terminal equipment.

Another lay-out would be the horizontal solution as sketched in Fig. 15b. This solution is favoured by certain HT generator manufacturers. Its main advantage lies in that one is more free in changing the generator stack length, i.e. the generator voltage without having to interfere with the ground level height. The tank can be placed on wheels; for access to the tube the tank can be retracted from it.

CONCLUSION

The results of the present investigation look encouraging. Further studies are required before one can determine the optimum design parameters to keep a good balance between improvement of the Linac beam quality and time, money and effort to achieve this goal.

Acknowledgments

We want to express our thanks to C.S. Taylor, Head of the Linac Group, for his support and to Messrs. P. Germain, H.G. Hereward, P. Lapostolle, P.H. Standley for their interest and their useful comments on our proposal.

References

[1] F. Vermeulen
Computer Simulation of Beam Bunching with Inclusion of Space Charge Forces and Quadrupole Lenses, MPS/Int. Lin 67-5.

[2] C.M. Turner
Physical Review, Vol. 81, 1951, p. 305 A.

[3] C.M. Turner
Bulletin of the American Physical Society, Vol. 1, 1956, p. 134.

[4] R. Herb
Handbuch der Physik, Vol. 44, 1959, p. 87.

[5] J. Blewett
Physical Review, Vol. 81, 1951, p. 305 A.

[6] C.M. Turner
The effects on pressure insulated electrostatic accelerators of ionization currents in the high pressure gas. (Unpublished)1955.

[7] J.L. McKibben
Bulletin of the American Physical Society Vol. 1, 1956, p.61.

[8] R.J. van de Graaff et al
Nature, Vol. 195, 1962, p. 1292.

[9] W.D. Allen
A new type of accelerating tube for electrostatic generators, NIRL/R/21, 1962.

[10] J.V. Kane
Review of Scientific Instruments, Vol. 37 1966, p. 555.

[11] L. Cranberg, J.B. Henshall
Journal of Applied Physics, Vol. 30, 1959, p. 708.

[12] I. Michael et al
Review of Scientific Instruments, Vol. 30, 1959, p. 855.

[13] Robinson, McIntosch, Nygard
Physical Review, Vol. 83, 1951, p. 233.

[14] J. Huguenin et al
Proceedings of 2nd and 3rd Int. Symp. on
Insulation of High Voltages in Vacuum,
Boston 1964 and 1966.

[15] F. Rohrbach et al
Proceedings of 2nd and 3rd Int. Symp. on
Insulation of High Voltages in Vacuum,
Boston, 1964 and 1966.

[16] B. Vosicki et al
Proceedings of 1966 Linear Accelerator
Conference, Oct. 1966.

[17] U. Tallgren
Progress Report on the CPS RF Ion Source
MPS/Int. LIN 66-8, Dec. 1966.

[18] L.C.W. Hobbis, L. Wroe
Ion Sources RHEL/M 125, April 1967.

[19] A. van der Schueren
Short Range Optical Link using Light
Emitting Gallium Arsenide Diodes and
Fotofets, MPS/Int. LIN 66-12.

[20] R. Vienet
Saturne, CEA Saclay, private communication.

[21] John G. Trump
US Particle Accelerators Conference,
Washington 1967, "New Developments in High
Voltage Technology", p. 113.

[22] C.S. Taylor, J. Huguenin, F. Block, F. Chiari
P. Têtu
CERN - PS 50 MeV Linac Progress Report
This Conference.

TABLE I

COMPARISON BETWEEN BIG DIAMETER TUBE WITH REENTRANT SOURCE AND/OR EARTH ELECTRODE AND SMALL DIAMETER TUBE WITH NO REENTRANCE

A. REENTRANT TUBE

Advantages	Disadvantages
1. Freedom in the choice of the accelerating gradient.	1. Important dimensions, therefore it follows:
2. Separation of the experimental researches of the different gradients.	a) Assembly procedures more difficult, especially in case of brazing
3. Insulator to metal junction screening as well as insulator screening can be made without getting higher gradients than the accelerating one.	b) More surfaces to degas (pump dimensions)
	c) More weight.
	2. Appearance of strong radial electrical fields, so need of a better screening of insulating walls against ions, electrons and rays.
	3. Ion Source: limited diameter, so design less easy, accessibility worse.
	4. Focusing or monitoring elements in the earth electrode: same difficulties as for the source.
	5. Separation valves between source and tube: difficult design because of limited diameter.

B. NON REENTRANT TUBE

Advantages and disadvantages are inverse to those of the reentrant tube.

FIG. 1 Typical I = f(E) curves of the PS linac

$E_y = E_z = E$

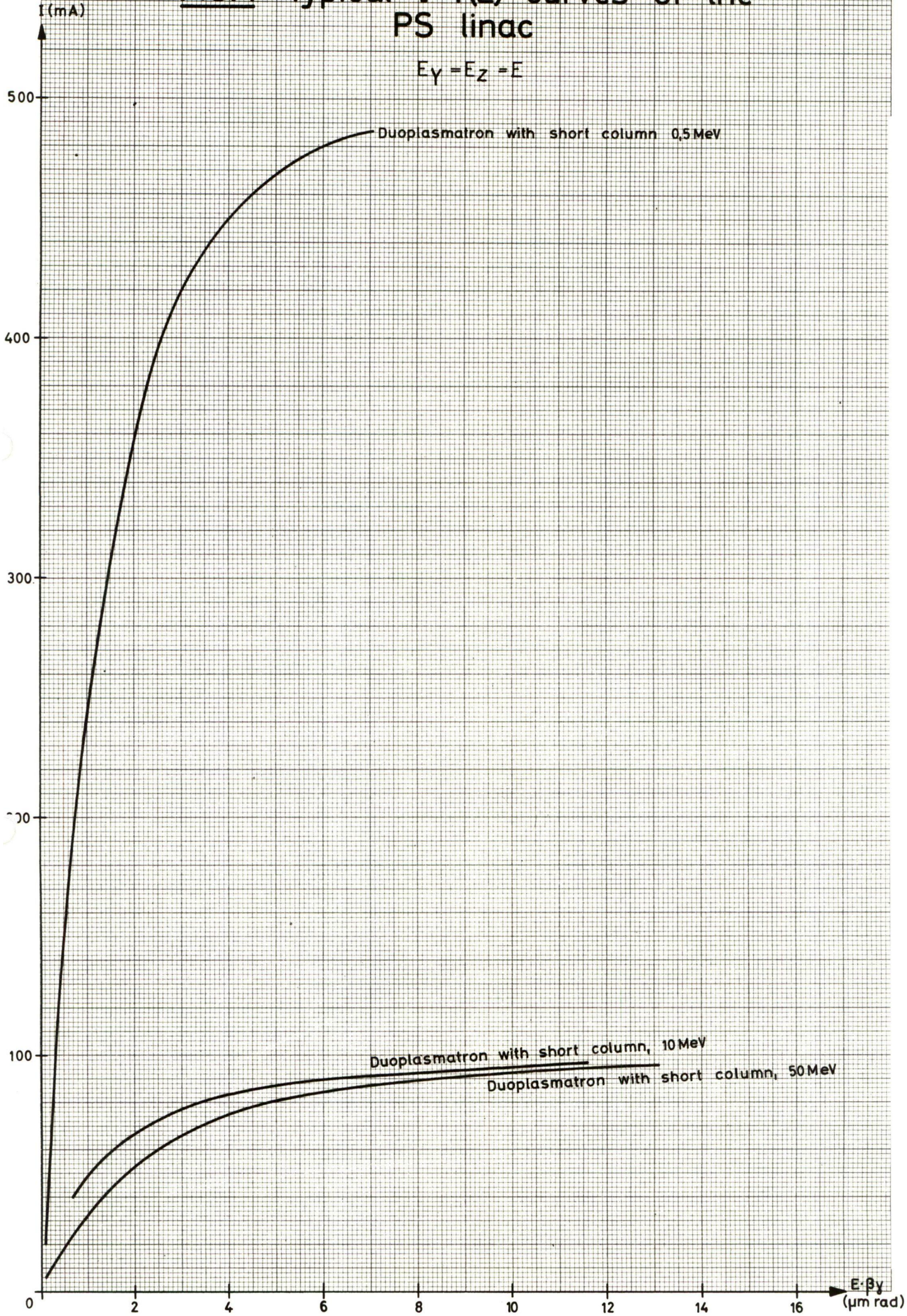

MPS 4158 · 105-1848-4 · 30.8.67 Z

FIG. 2 Energy increase in the 1st tank

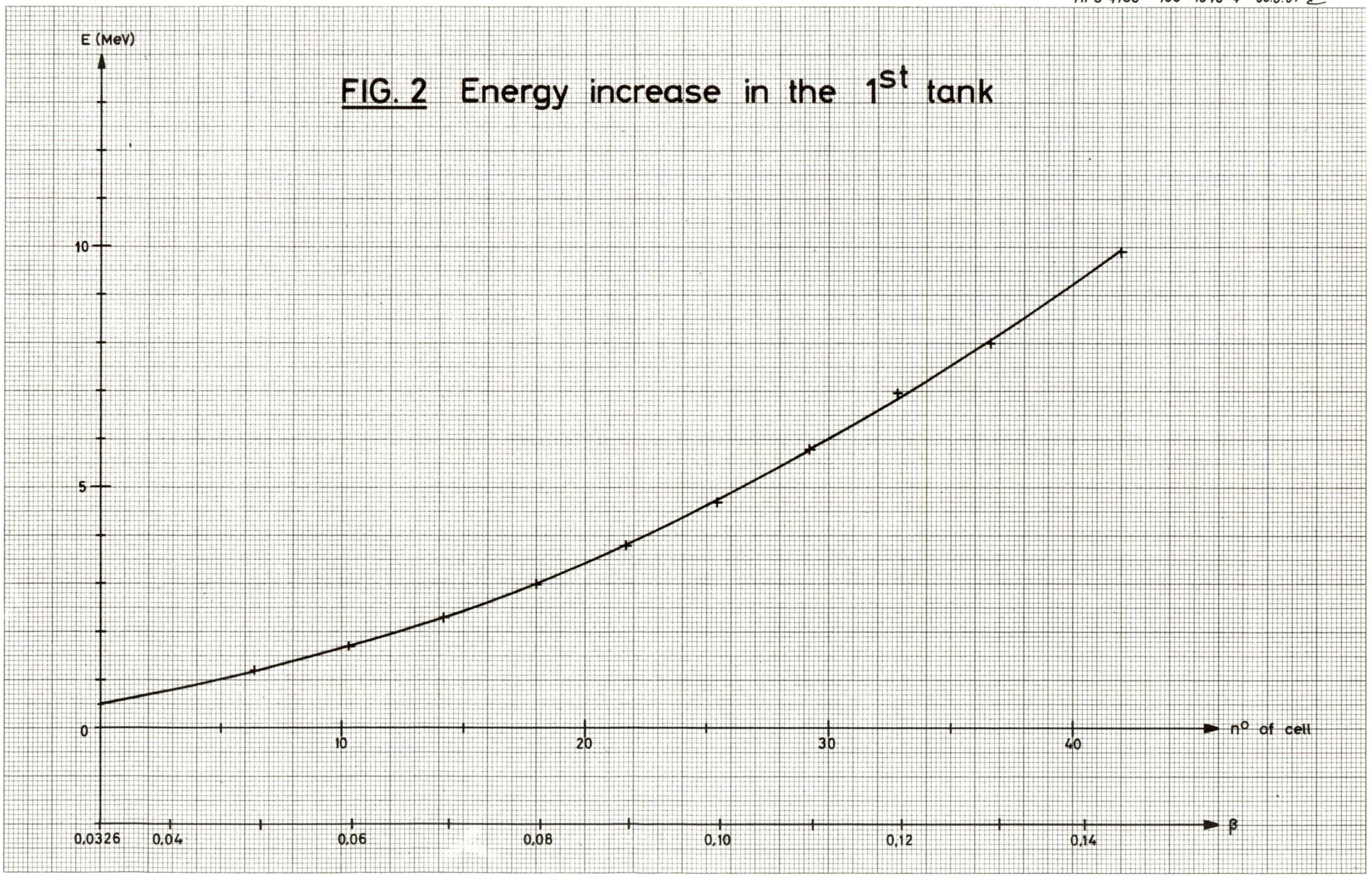

MPS 4158 · 105-1849-4 · 30.8.67

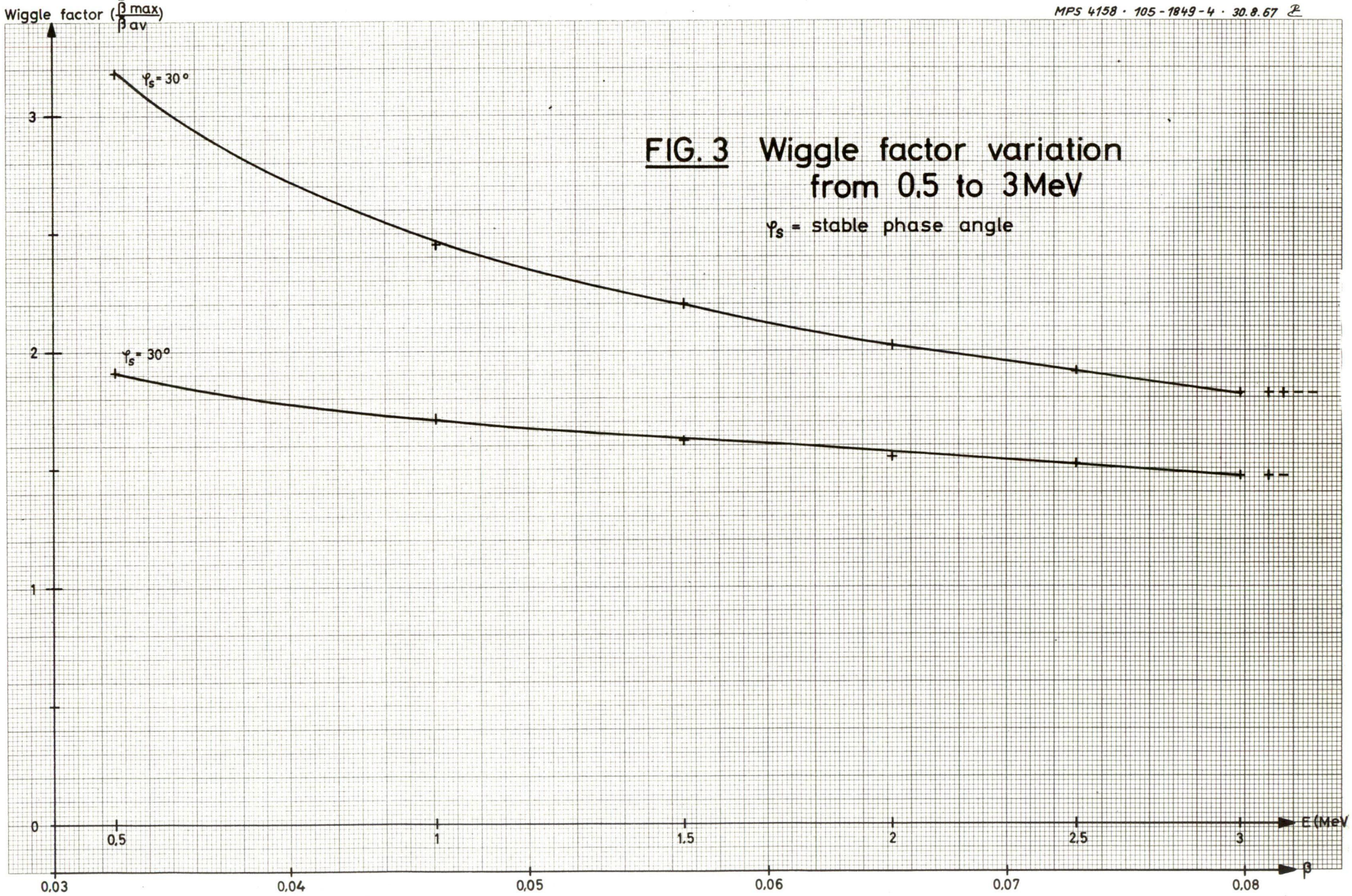

FIG. 3 Wiggle factor variation from 0.5 to 3 MeV

φ_s = stable phase angle

MPS 4158 • 105-1850-4 • 30.8.67 E

FIG. 4 Drift tube bore radius and gap length in the first part of tank 1

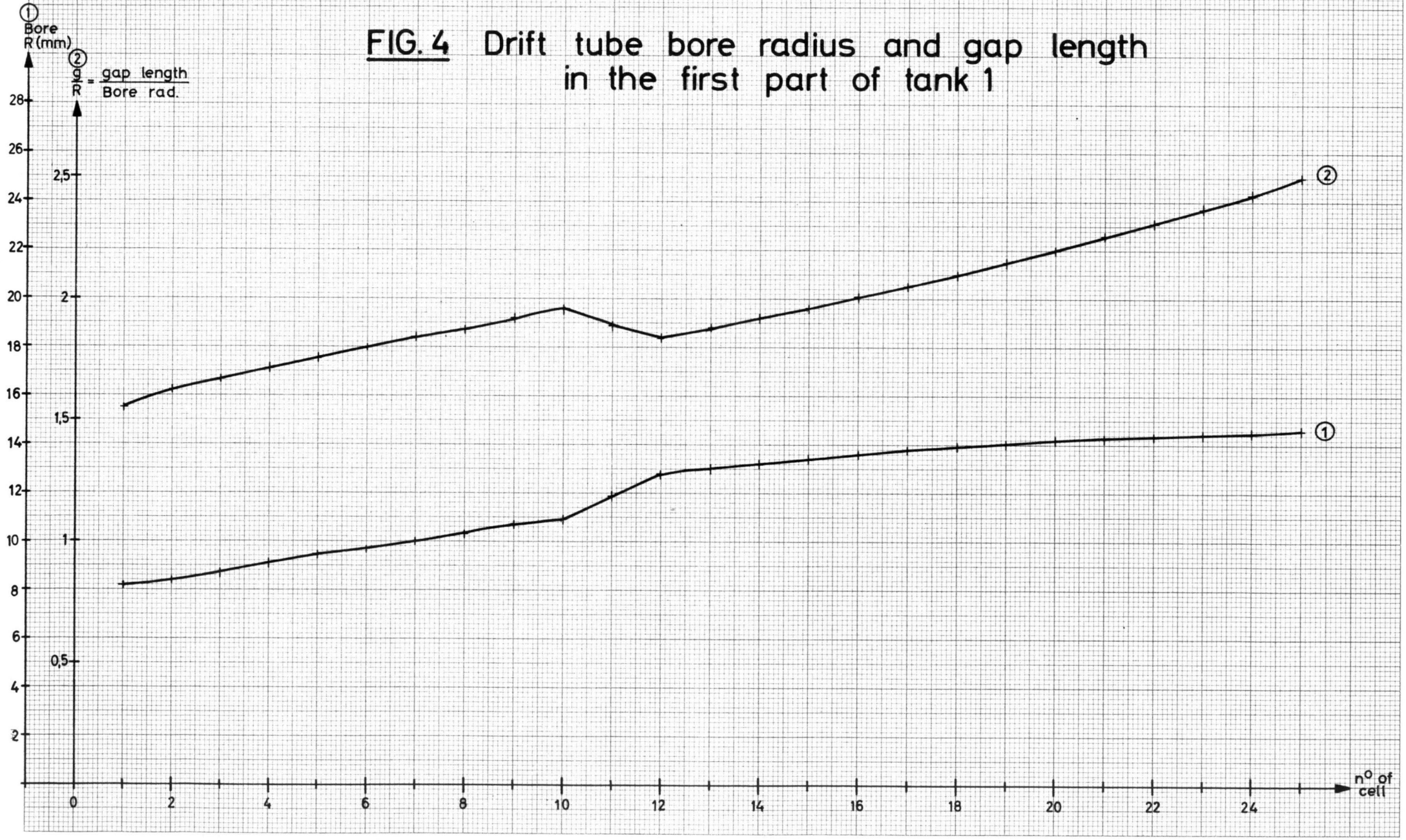

FIG. 5 Variation of $\bar{\beta}_{max}$

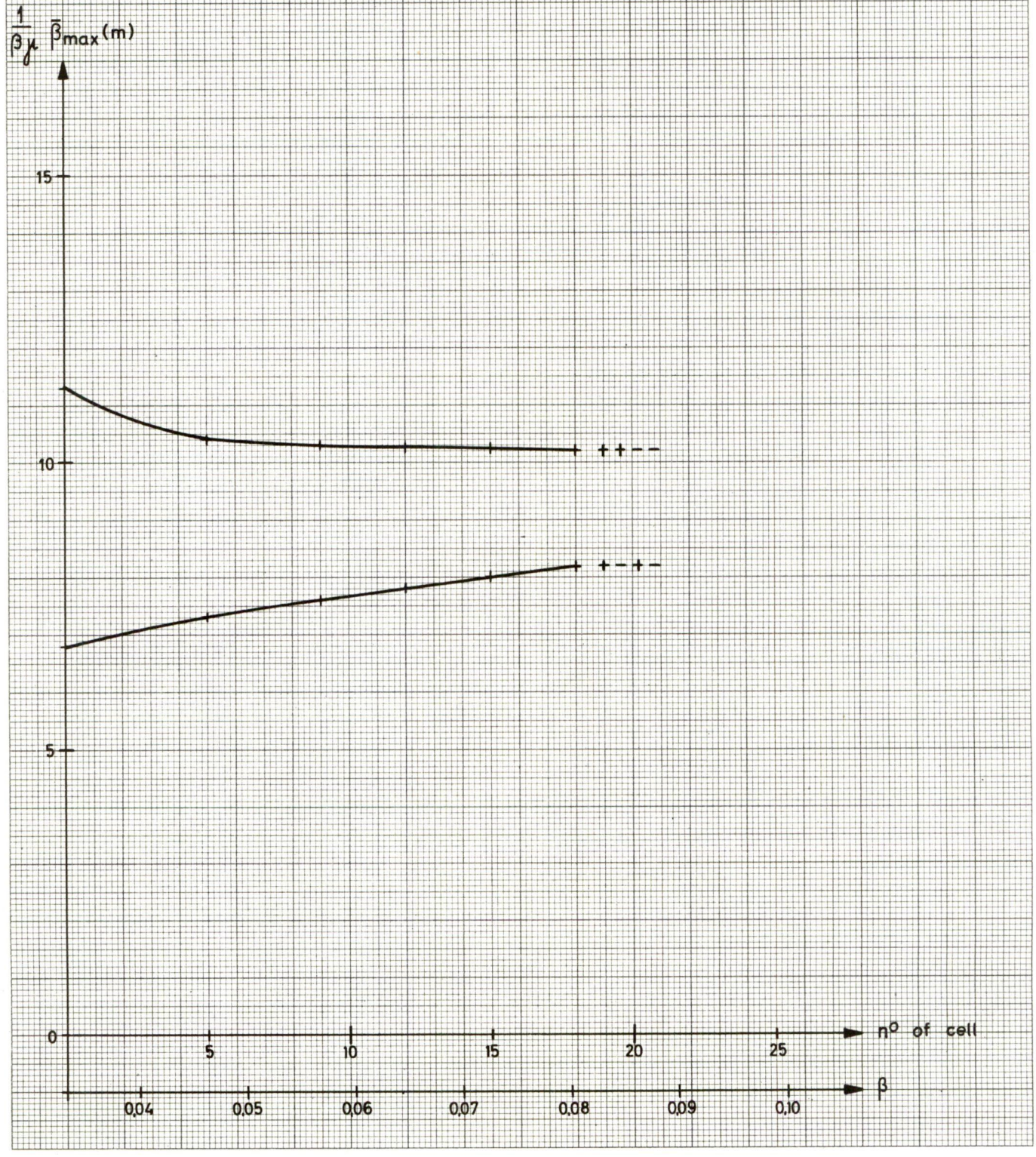

FIG. 6 Variation of the linac acceptance, normalized to the value at 0,5 MeV and ++-- focusing structure

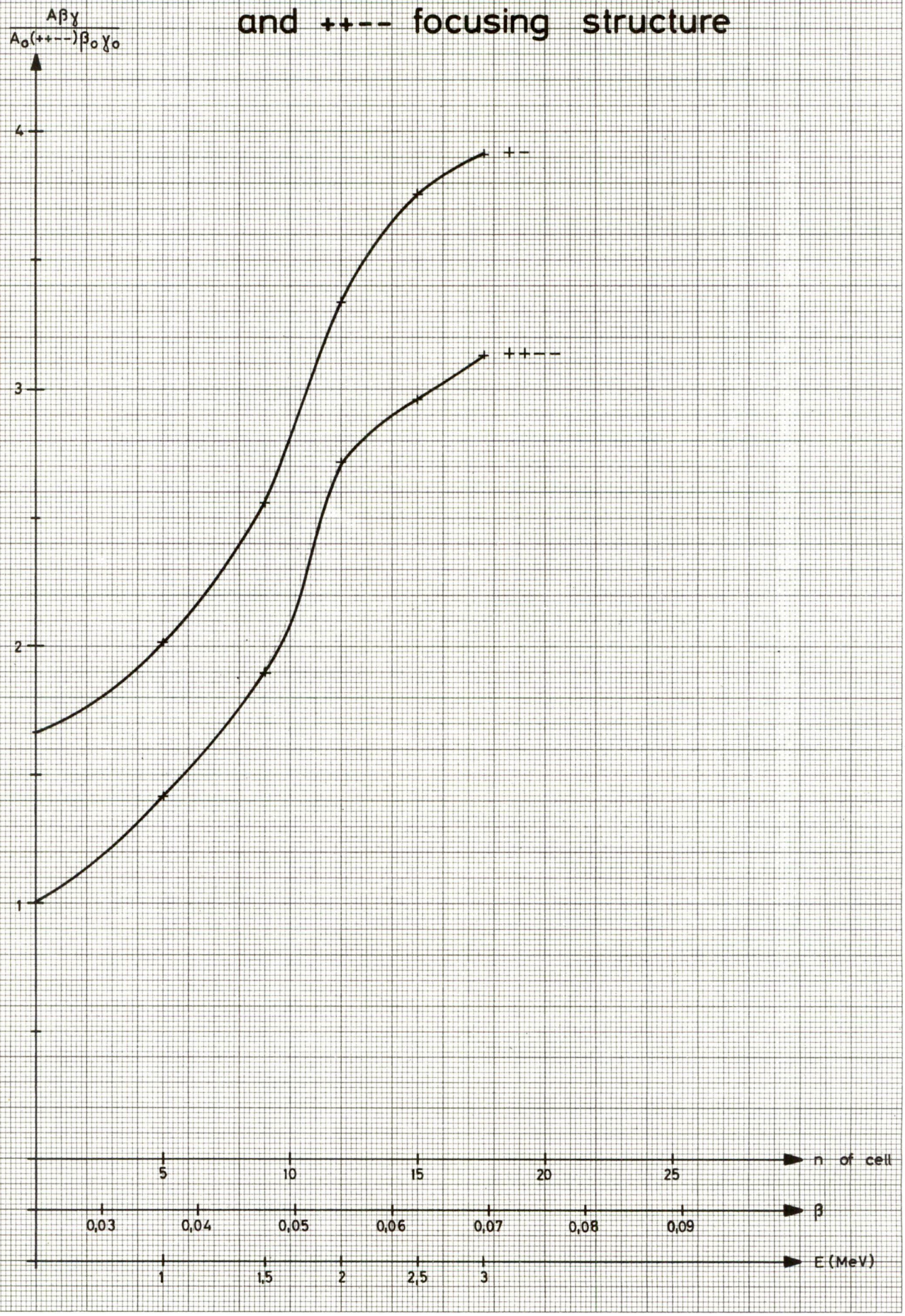

MPS 4158 · 105 - 1853 - 4 · 30.8.67

FIG. 7 Quadrupole lens strength in thin lens approximation

δ is expressed in the normalized $\left(\frac{r}{p}\right)$ system as $\delta = \varphi \frac{e\beta\lambda \frac{\partial B}{\partial r}}{m_o c}$

φ = filling factor

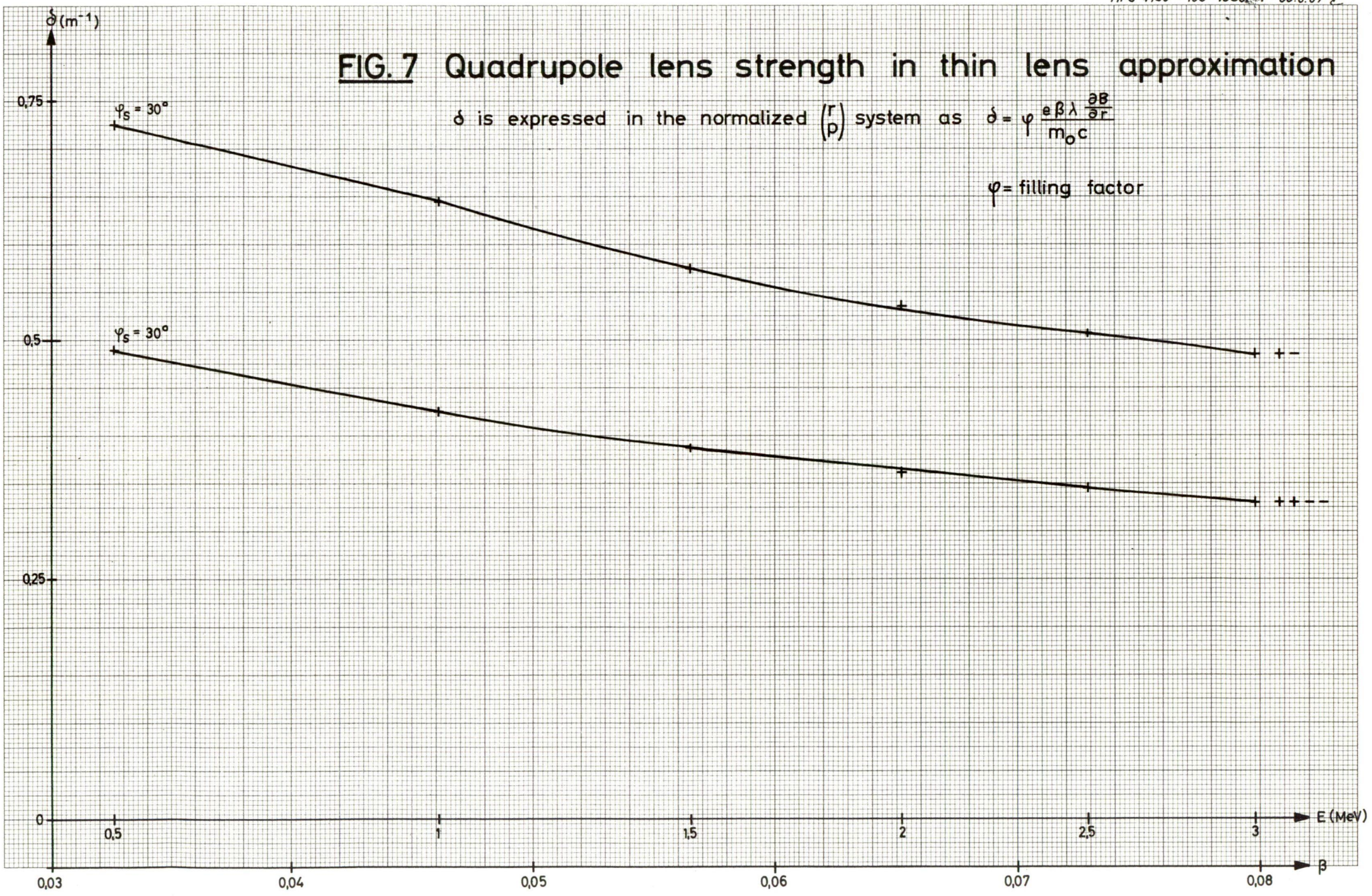

MPS 4158 · 105 - 1854 - 4 · 30.8.67 E

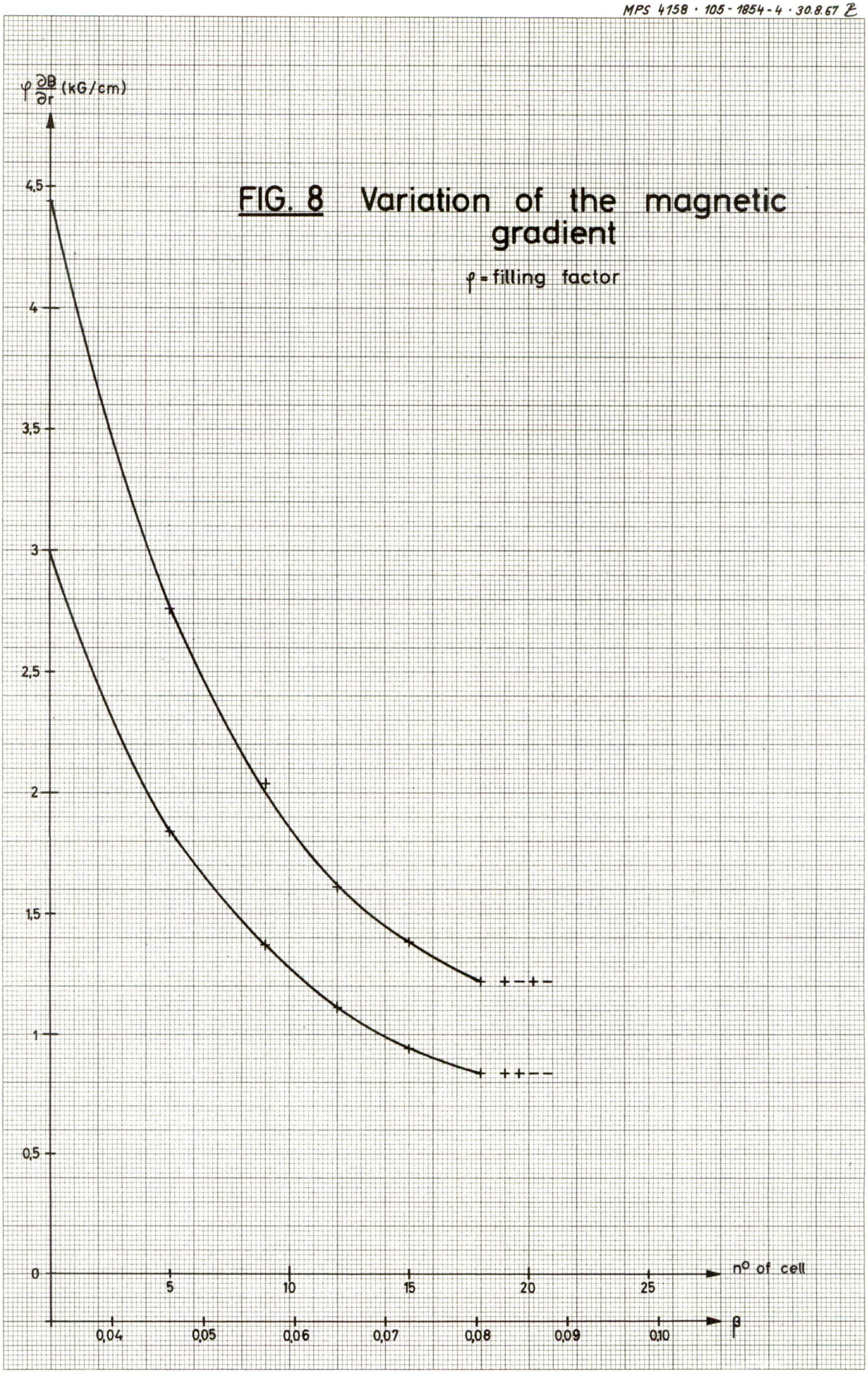

FIG. 8 Variation of the magnetic gradient

φ = filling factor

FIG. 9 Ratio of gap defocusing to quadrupole lens strength

(all in thin lens approximation)

f = RF frequency

gap defocusing: $\frac{d^2r}{dt^2} - \chi^2 r = 0$

$q = \frac{\Omega r}{\Omega \varphi} = 0{,}75$

$\varphi_s = 30°$

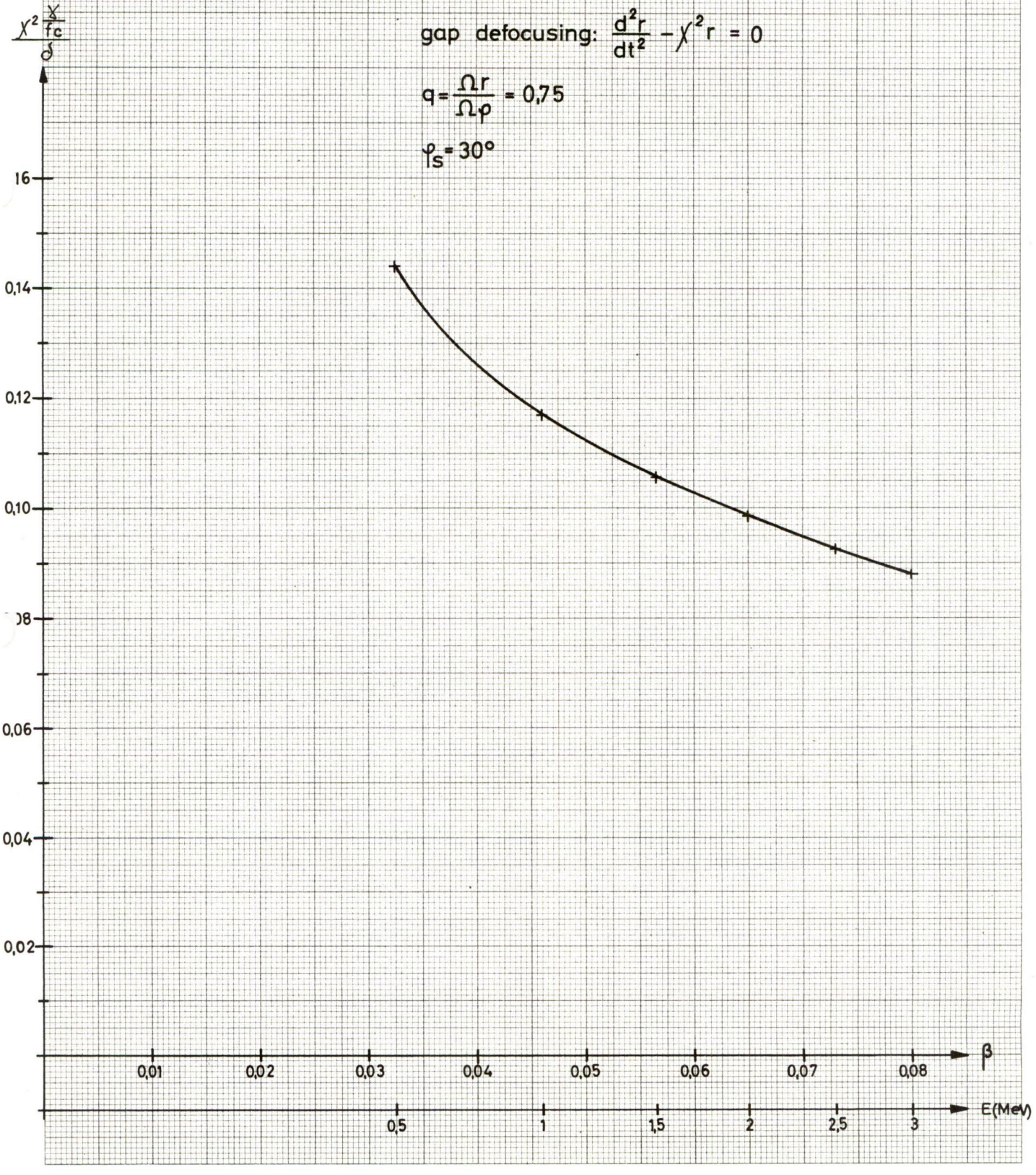

FIG. 10 Quadrupole strength as function of $q = \frac{\Omega r}{\Omega \varphi}$

Injection energy = 2,5 MeV

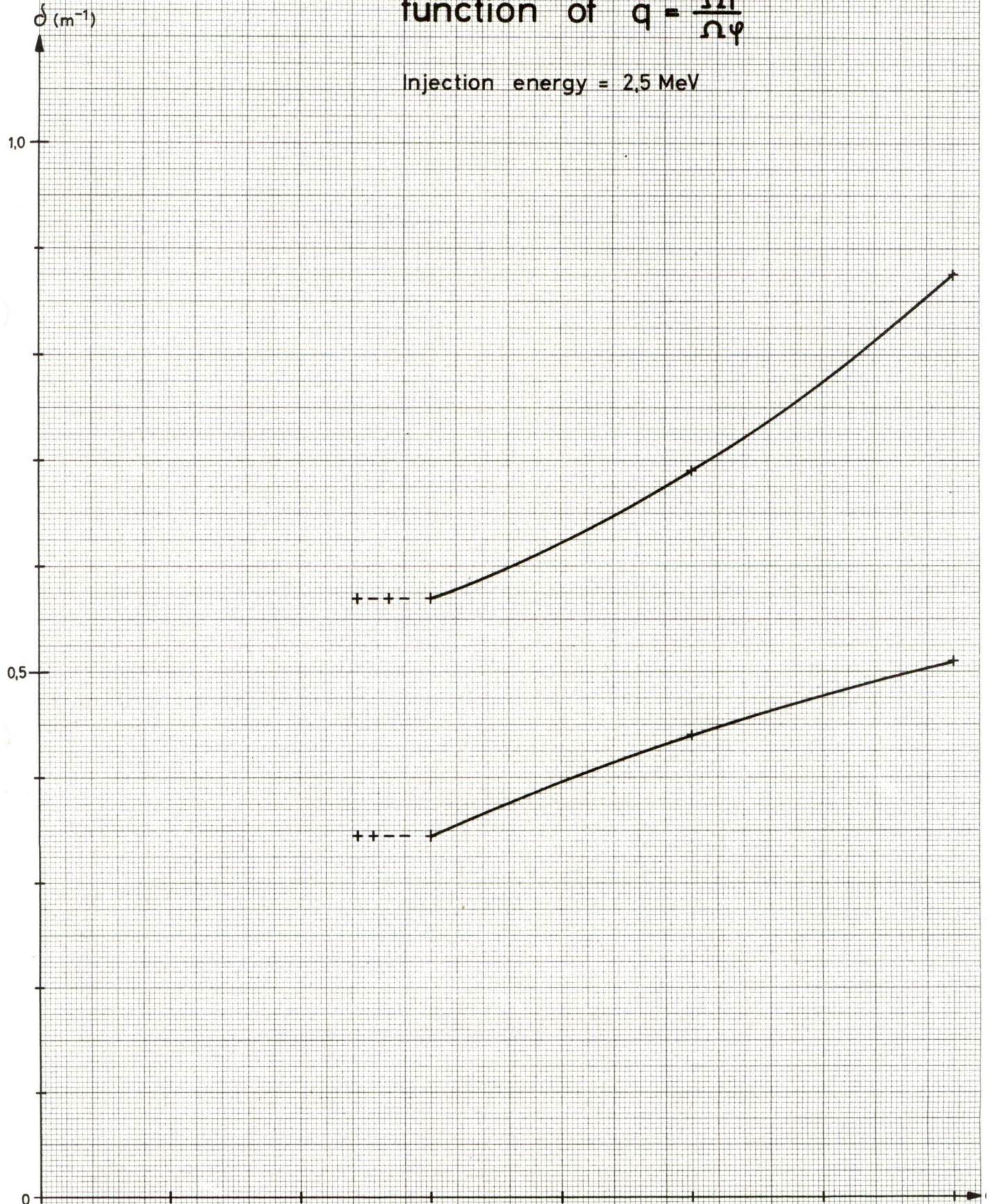

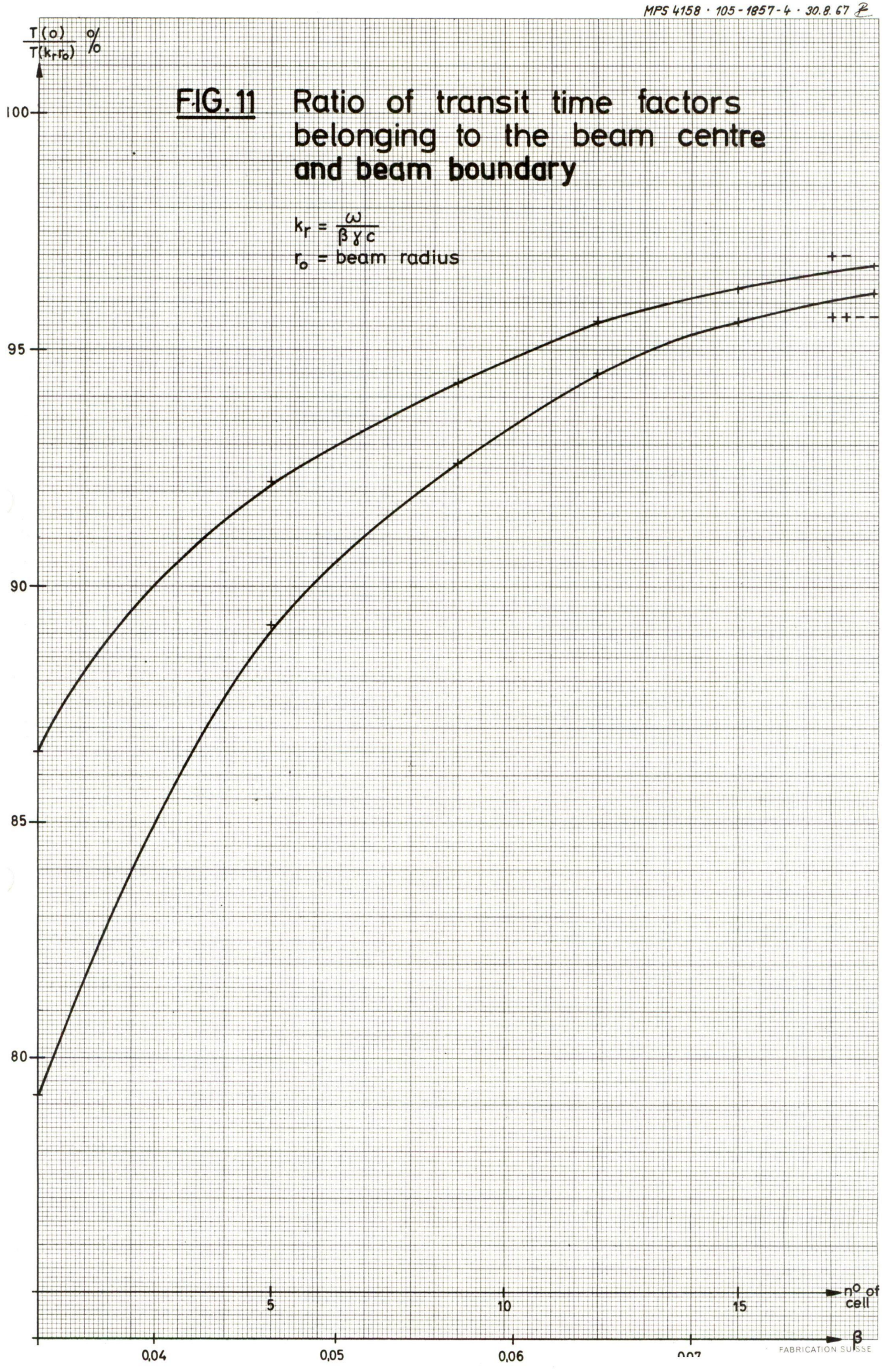

FIG. 11 Ratio of transit time factors belonging to the beam centre and beam boundary

$k_r = \frac{\omega}{\beta \gamma c}$

r_o = beam radius

MPS 4158 · 105 - 1858 - 4 · 20.10.67

FIG. 12 Effect of bunching

Percentage of particles within a phase interval $\pm\Delta\phi$.

E = 0,530 MeV

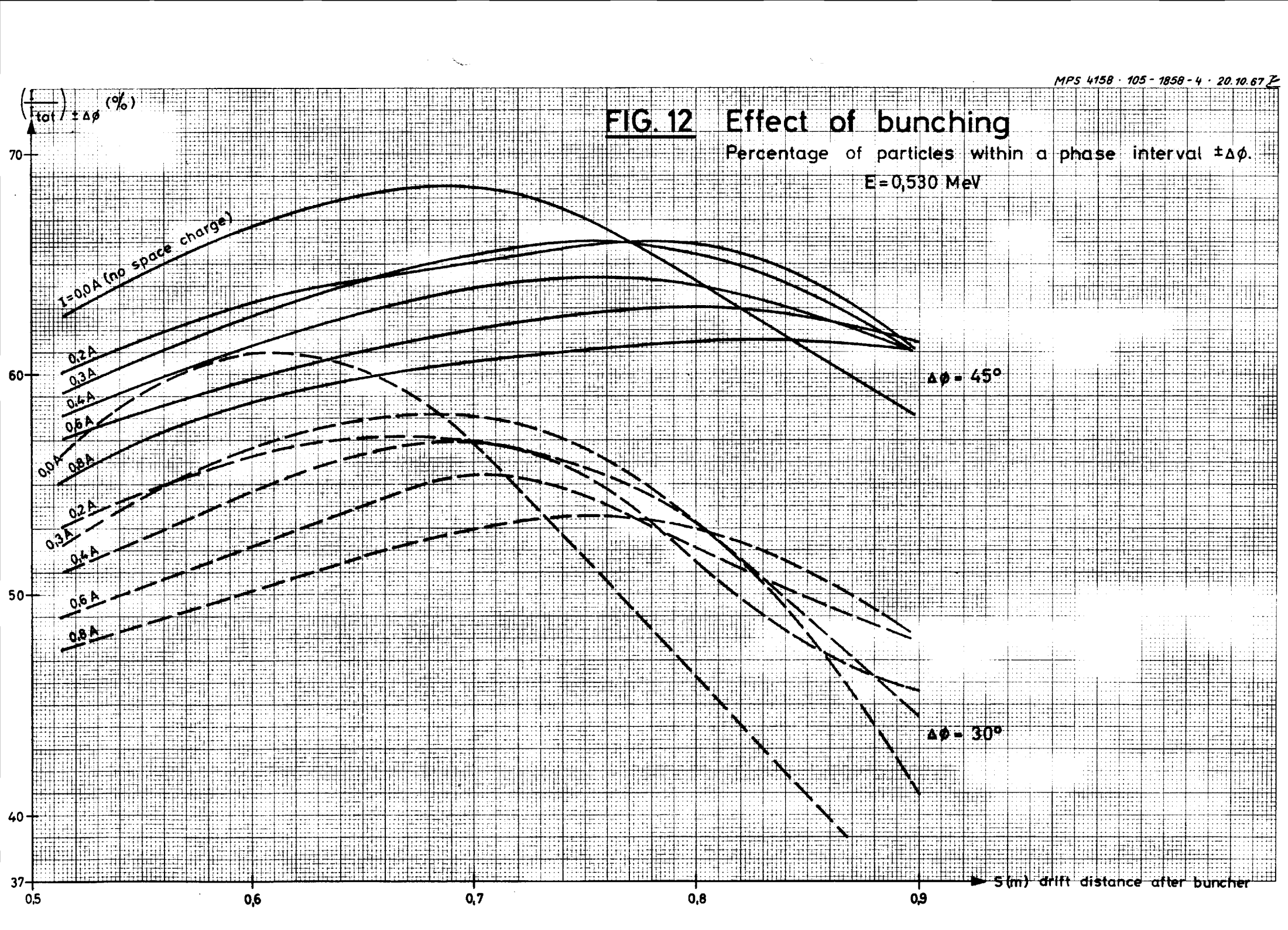

MPS 4158 · 105 - 1858 - 4 · 20.10.67

FIG. 12a Effect of bunching

Increase in beam radius due to buncher gap defocusing and space charge forces.

E = 0,530 MeV

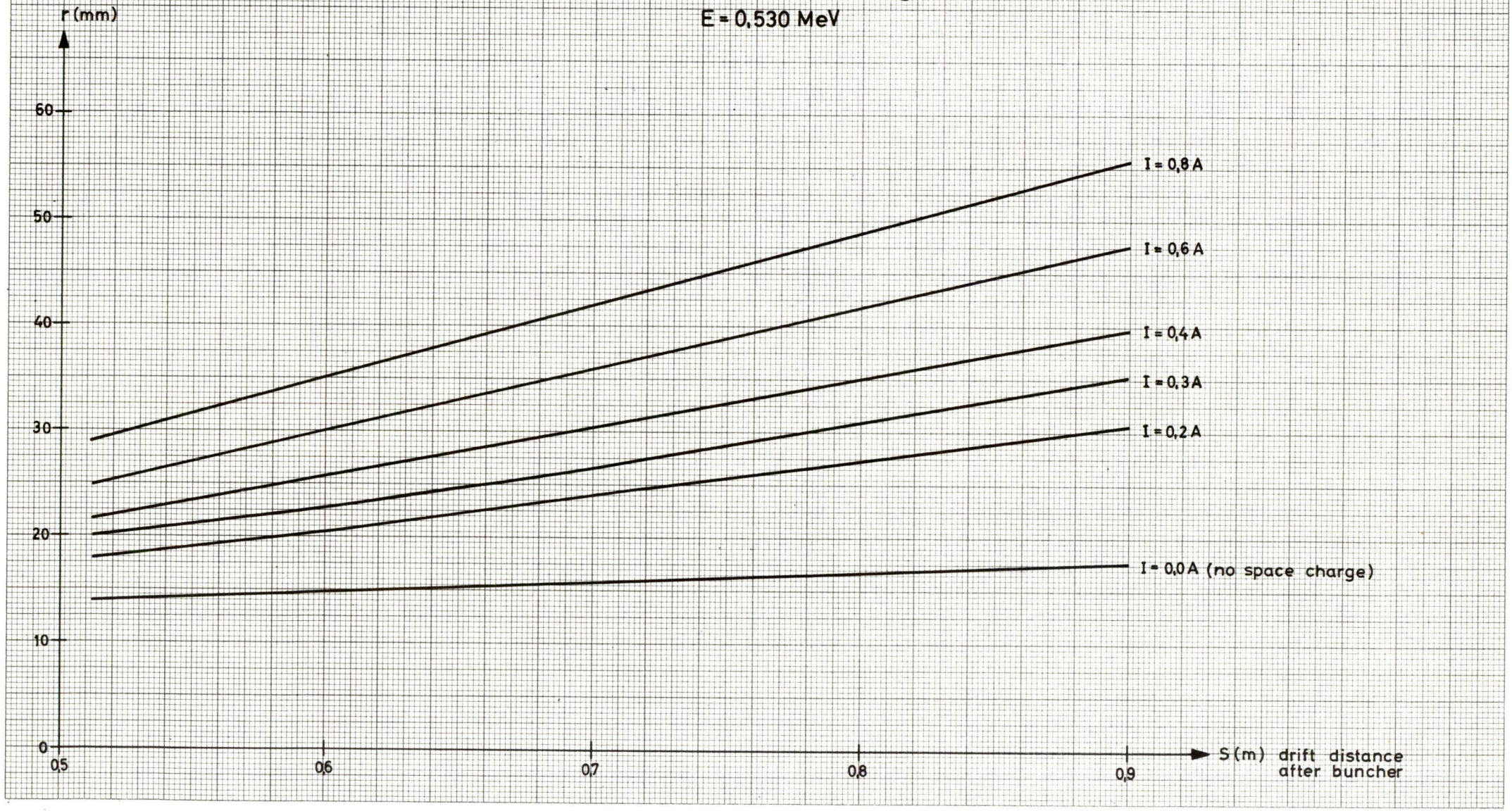

MPS 4158 · 105 - 1859 - 4 · 20.10.67 B

FIG. 13 Effect of bunching

Percentage of particles within a phase interval $\pm \Delta\phi$. E = 2,5 MeV

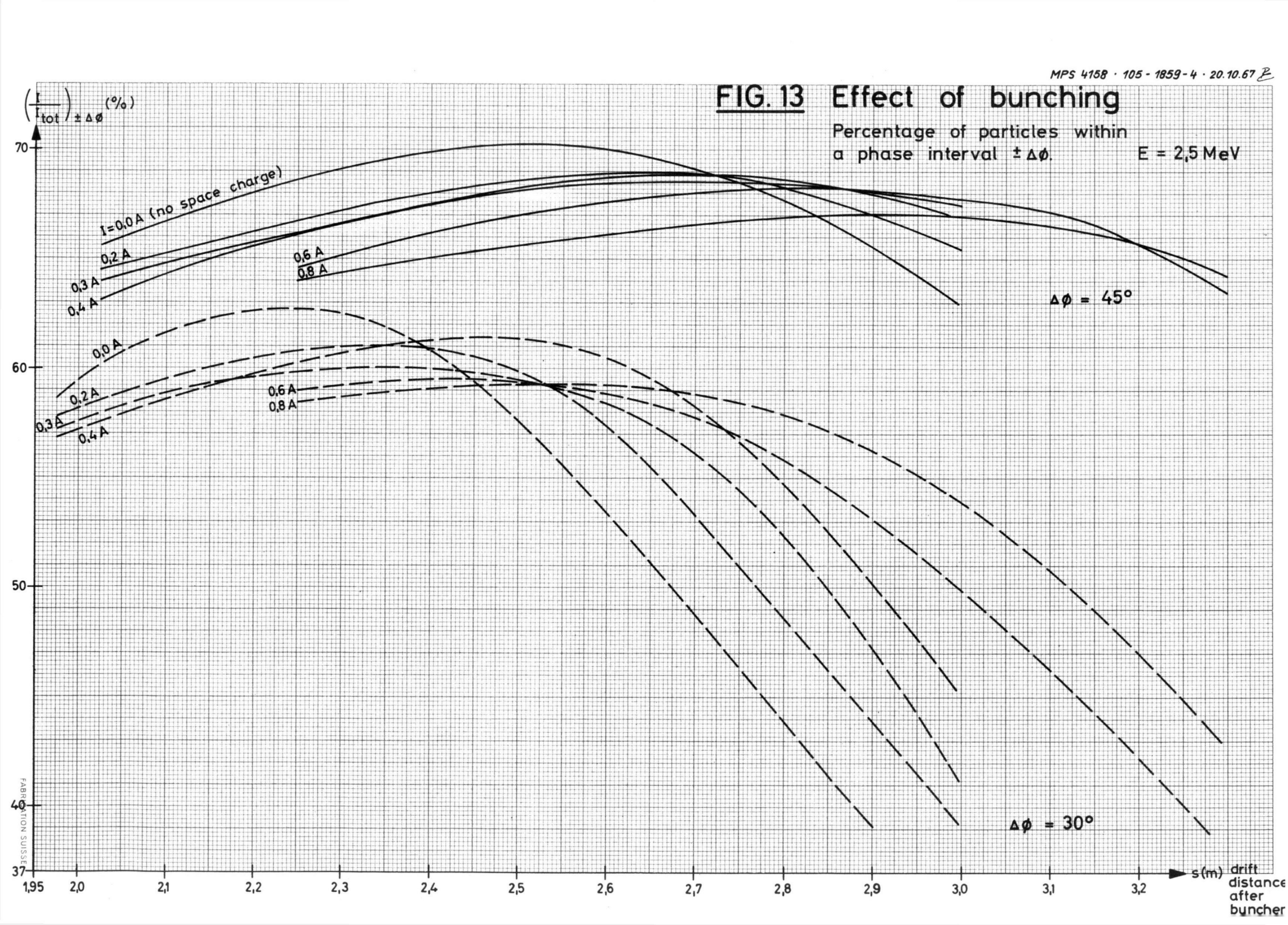

MPS 4158 · 105 - 1859 - 4 · 20.10.67

FIG. 13a Effect of bunching

Increase in beam radius due to buncher gap defocusing and space charge forces.

E = 2,5 MeV

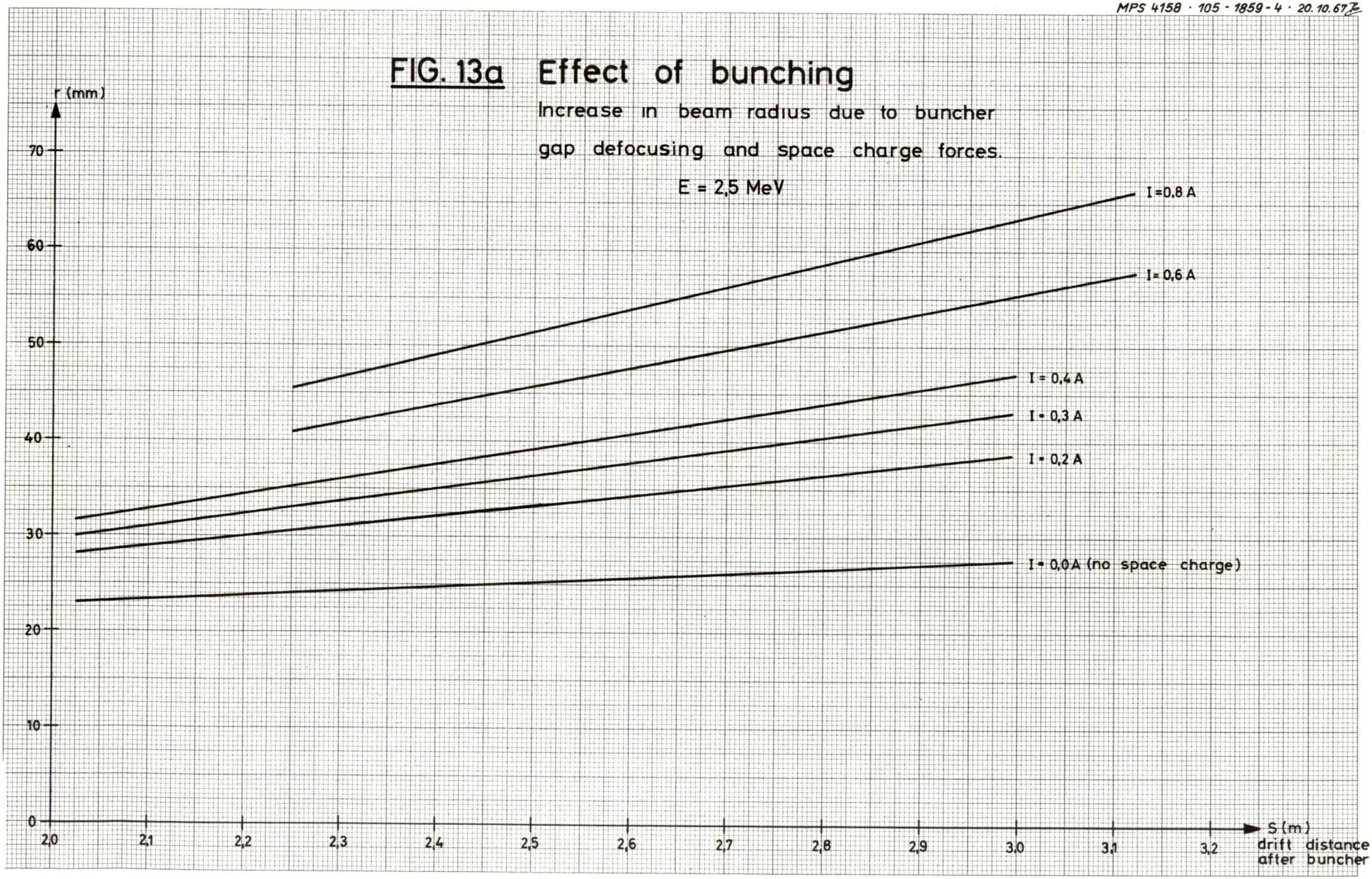

FIG. 14 Bunching quality factor η

$$\eta = \frac{\left(\frac{I}{I_{tot}}\right)_{max \pm 45°}}{\frac{r_{I\,max} - r_{o\,max}}{r_{o\,max}}}$$

$r_{I\,max}$ — beam radius for current I at position of maximum bunching

$r_{o\,max}$ — as above, but for I = 0 (no space charge)

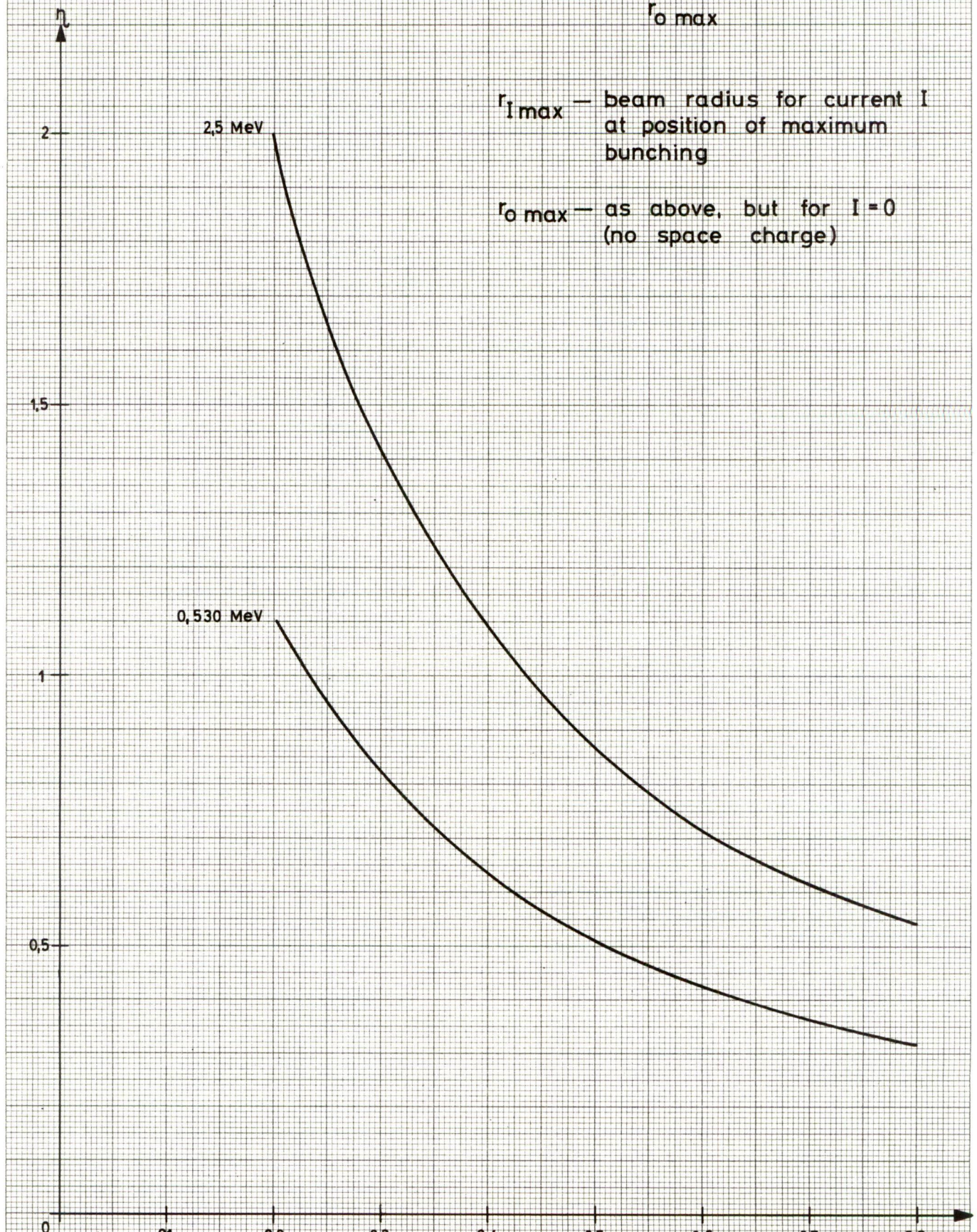

FIG. 15 Possible physical arrangement of generator and tube

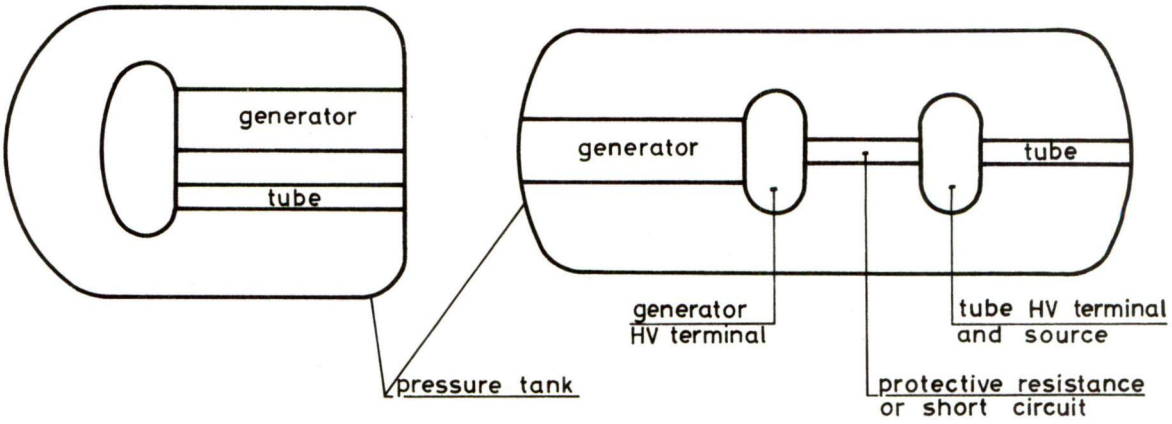

a) parallel layout

b) series layout

MPS 4158 · 105 - 1829 - 4 · 21.7.67 R

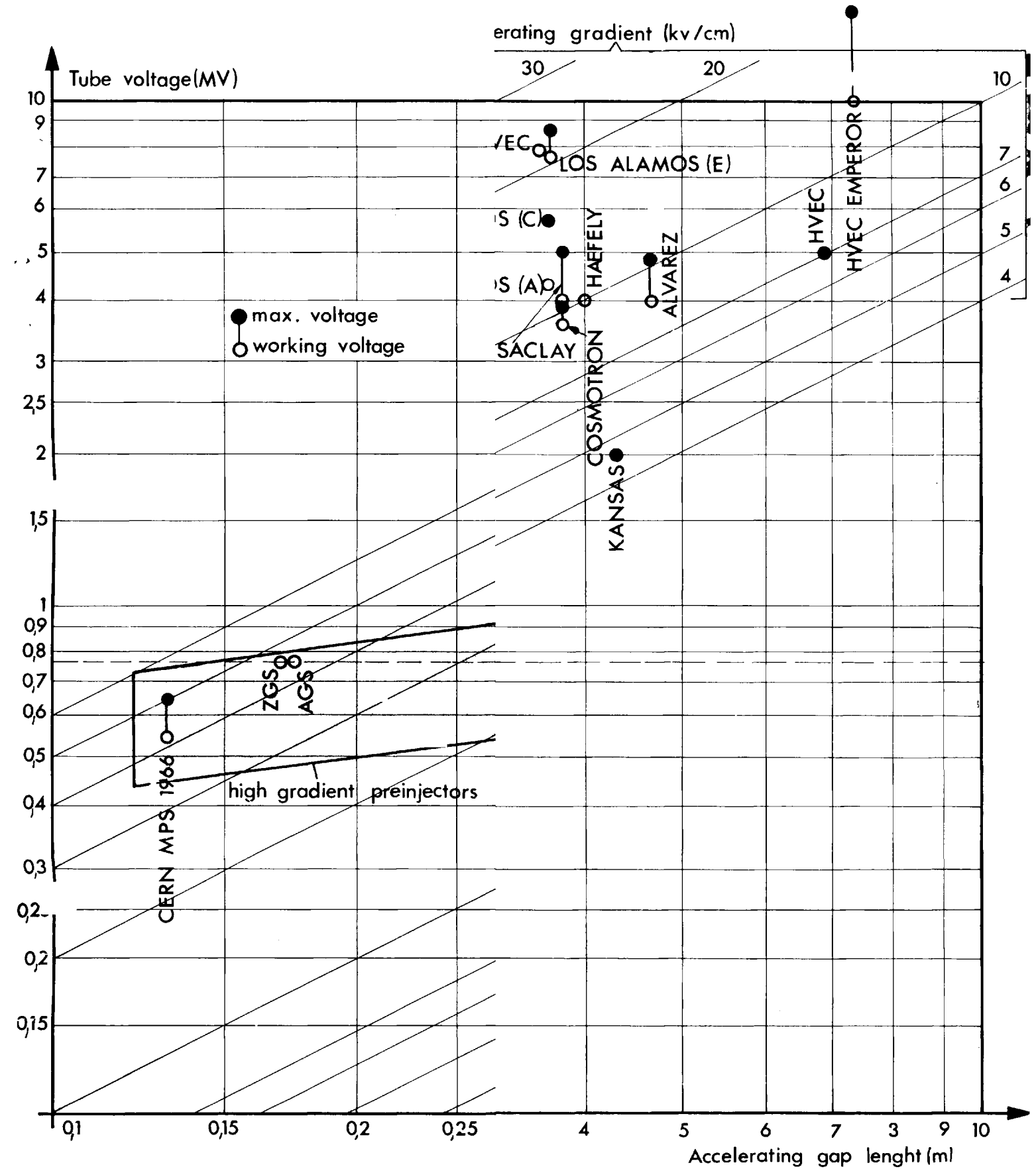

nd accelerating gradient

1833-3 15-5-68

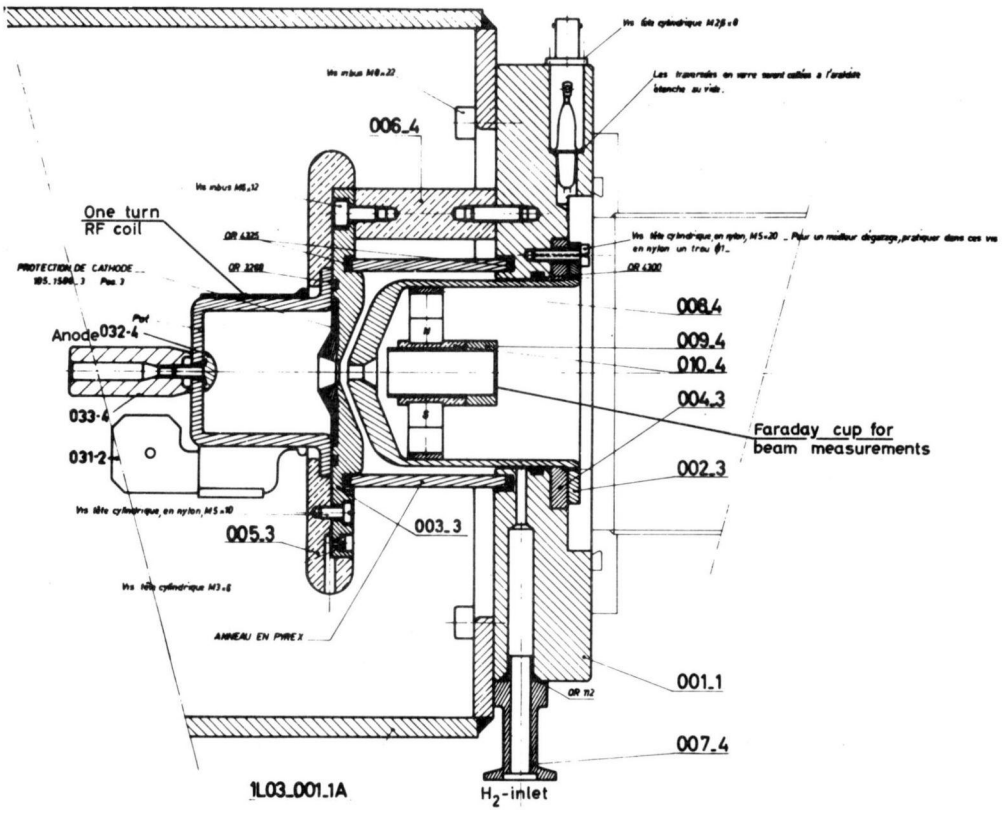

FIG. 17 Layout of experimental RF ion source with two step acceleration before outlet hole.

FIG.18 Example of miniaturisation of grid - pulsed RF - oscillator for ion source

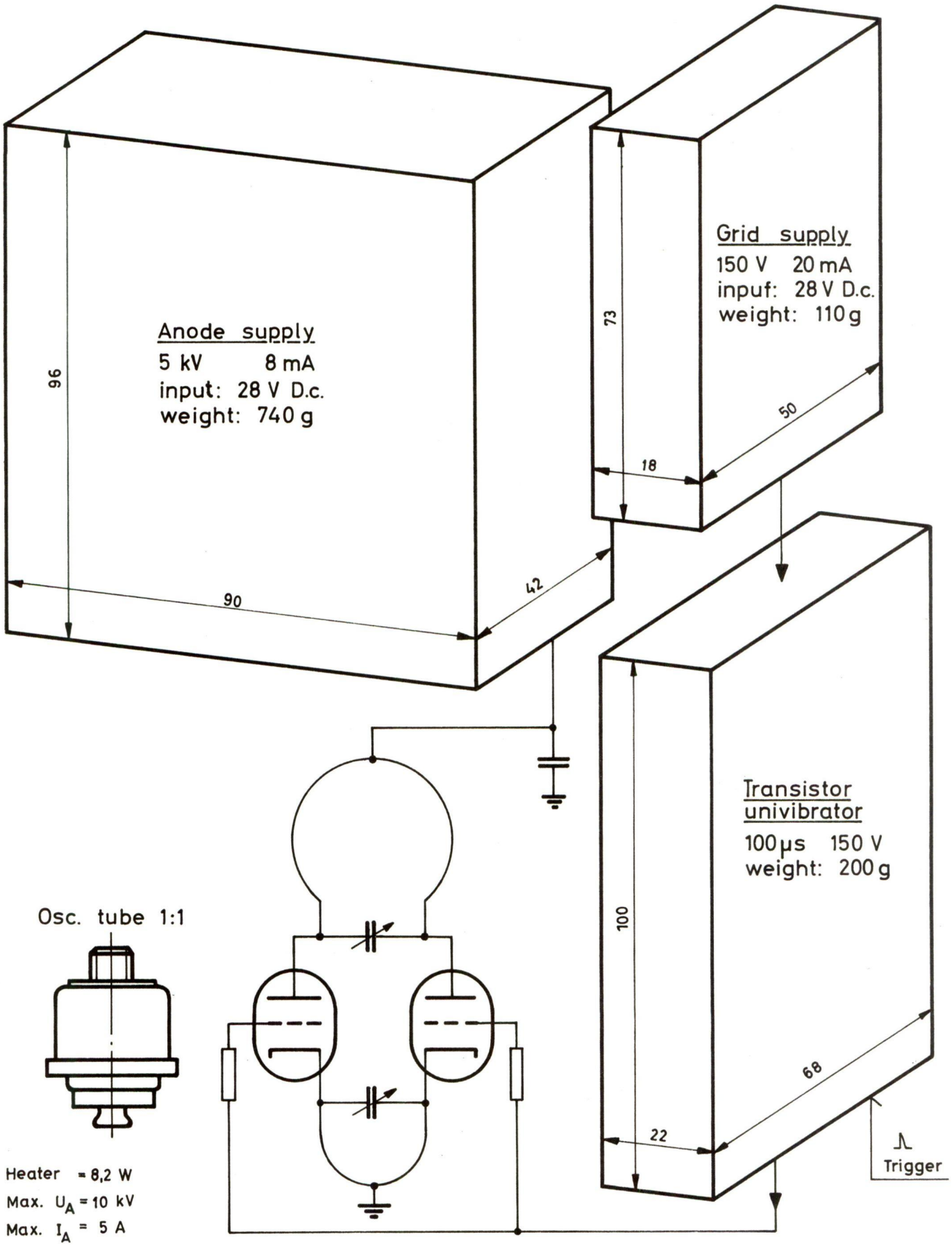

FIG. 19 : Example of a possible vertical lay-out of the preinjector HT - generator

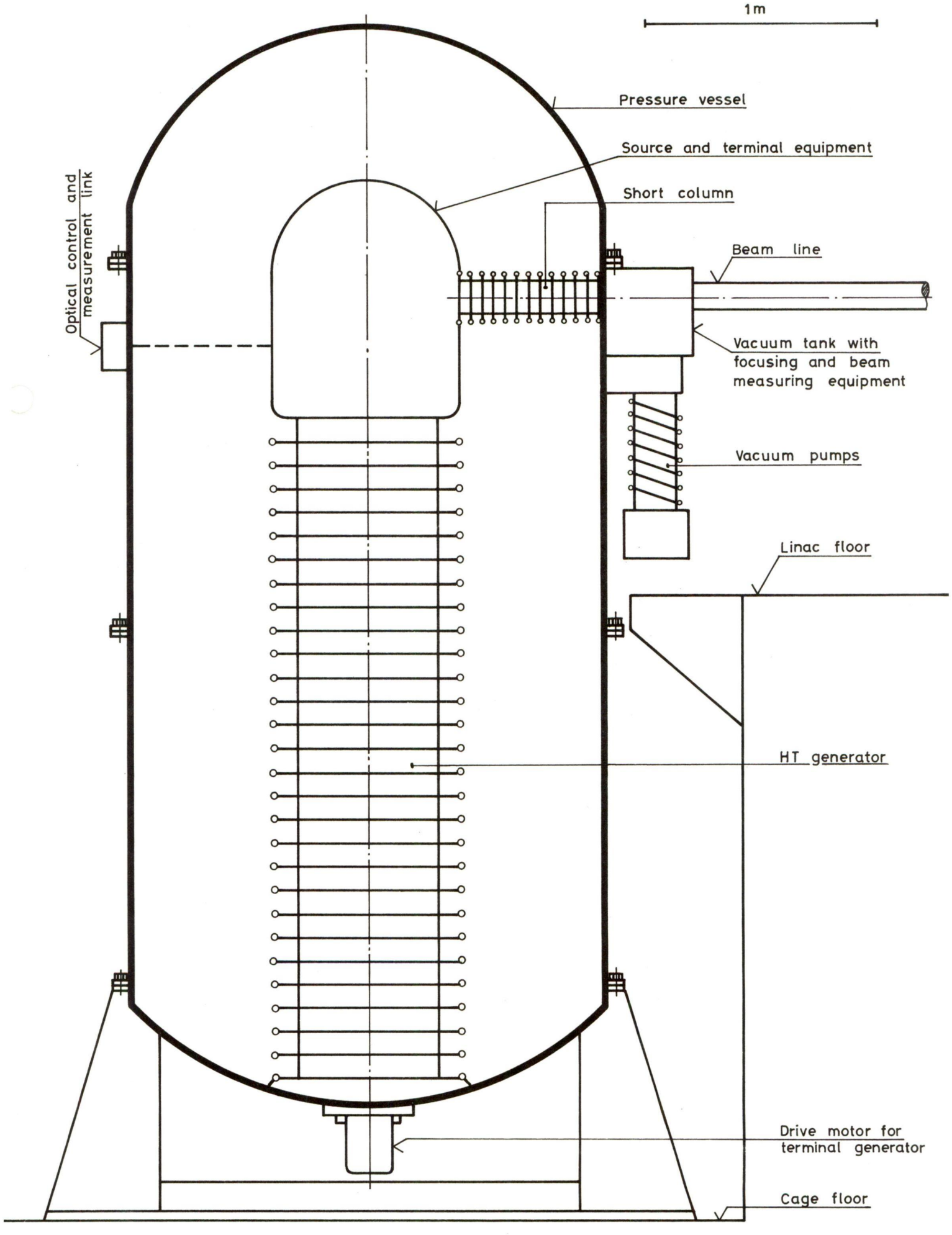

MPS 4158 · 105 - 1873 - 4 · 22. 10. 67